MILLIMETER-WAVE BISTATIC RADAR SCATTERING FROM TERRAIN

FINAL REPORT

U.S. Army Research Office
Box 12211
Research Triangle Park, NC 27709

Contract DAAL03-92-G-0190
July, 1995

APPROVED FOR PUBLIC RELEASE, DISTRIBUTION UNLIMITED

Fawwaz T. Ulaby

MILLIMETER-WAVE BISTATIC RADAR SCATTERING FROM TERRAIN

FINAL REPORT
U.S. ARMY RESEARCH OFFICE
CONTRACT DAAL03-92-G-0190
July, 1995

MASTER COPY KEEP THIS COPY FOR REPRODUCTION PURPOSES

REPORT DOCUMENTATION PAGE

Form Approved
OMB No. 0704-0188

1. AGENCY USE ONLY (Leave blank)	2. REPORT DATE	3. REPORT TYPE AND DATES COVERED
	]995, July 24	Final 6-]-92 - 5-3]-95

4. TITLE AND SUBTITLE
MILLIMETER-WAVE BISTATIC RADAR SCATTERING FROM TERRAIN

5. FUNDING NUMBERS

6. AUTHOR(S)
Fawwaz T. Ulaby

7. PERFORMING ORGANIZATION NAME(S) AND ADDRESS(ES)
Radiation Laboratory, University of Michigan
Ann Arbor, Michigan 48]09

8. PERFORMING ORGANIZATION REPORT NUMBER
02953]-]-F

9. SPONSORING/MONITORING AGENCY NAME(S) AND ADDRESS(ES)
U. S. Army Research Office
P. O. Box 12211
Research Triangle Park, NC 27709-2211

10. SPONSORING/MONITORING AGENCY REPORT NUMBER
DAAL03-92-G-0190

11. SUPPLEMENTARY NOTES
The view, opinions and/or findings contained in this report are those of the author(s) and should not be construed as an official Department of the Army position, policy, or decision, unless so designated by other documentation.

12a. DISTRIBUTION/AVAILABILITY STATEMENT
Approved for public release; distribution unlimited.

12b. DISTRIBUTION CODE

13. ABSTRACT *(Maximum 200 words)*

This final report provides a summary of the results realized over the past 3 years with regard to the characterization of bistatic radar scattering from terrain. The papers and report published under this program describe hardware and techniques developed for bistatic measurements, and an enhancement to the Physical Optics model for surface scattering.

14. SUBJECT TERMS
radar scattering, terrain clutter

15. NUMBER OF PAGES

16. PRICE CODE

17. SECURITY CLASSIFICATION OF REPORT	18. SECURITY CLASSIFICATION	19. SECURITY CLASSIFICATION OF ABSTRACT	20. LIMITATION OF ABSTRACT
UNCLASSIFIED	UNCLASSIFIED	UNCLASSIFIED	UL

NSN 7540-01-280-5500

Standard Form 298 (Rev. 2-89)
Prescribed by ANSI Std. Z39-18
298-102

1 Introduction

A program for measuring the bistatic scattering of microwaves from rough surfaces has been conducted for the purpose of understanding the nature of the role of bistatic scattering in the radar backscatter response of complex scenes such as forests and crops. A Bistatic Measurement Facility, an automated radar system operating with a center frequency of 9.25 GHz, has been designed and built for measuring the bistatic scattering response of rough surfaces in a laboratory setting. In addition, an enhancement to the Physical Optics model for surface scattering has been developed.

This report provides a summary of the results realized under this program, with the details provided in Appendix A in the form of reprints of articles published in scientific journals and symposia proceedings. Not included in the Appendix is a long report [1] documenting the operation and maintenance of the Bistatic Measurement Facility, created for use by the U.S. Army Waterways Experiment Station. These reports have been requested by and provided to numerous U.S. Army and other DOD groups and laboratories. The references cited in the body of this report refer to the publication list given in Section 3.

2 Summary of Results

Previous research, which resulted in the development of the Michigan Microwave Canopy Scattering (MIMICS) model, demonstrated that an important mechanism for describing the radar scattering from complex natural targets, such as forests and crops, involves a double bounce of energy involving both the ground and overstructure components, such as stems, branches, trunks and/or the canopy. In order to understand this double bounce mechanism, the individual bistatic scattering mechanisms at the ground and the overstructure components can be explored individually. This report contains the results of our efforts to understand the nature of bistatic scattering from the ground.

2.1 Bistatic Measurement Facility

While extensive theoretical developments exist regarding bistatic scattering, experimental confirmations are very scarce, and therefore an emphasis was placed on developing an accurate means of measuring the bistatic scattering from the ground. From our experience with previous efforts to make such measurements, a Bistatic Measurement Facility has been designed from scratch and is now in operation. Critical design considerations include main-

taining polarization purity, polarimetric calibration, positional and angular accuracy, large numbers of independent samples, automation for acquiring large data sets, and long term stability.

A second Bistatic Measurement Facility has been designed and built for the U.S. Army Waterways Experiment Station and is awaiting delivery pending the preparation of appropriate laboratory space at WES.

2.2 An extension to Physical Optics

One of the oldest and most popular rough surface scattering models is the Physical Optics model. An extension of the model, involving higher order slope dependence, has been developed and confirming measurements in the specular direction have been made on the Bistatic Measurement Facility. These results are published in [2, 3]. The first experimental evidence of Brewster angle migration toward nadir as the surface roughness increases, predicted by the Small Perturbation Method, is also contained in this paper.

3 List of Publications

References

[1] R. De Roo, R. Hartikka, N. Peplinski, and A. Zambetti, "Bistatic measurement facility user's manual," Technical Report 031163-F, The University of Michigan, Ann Arbor, MI, August 1994.

[2] R. D. De Roo and F. T. Ulaby, "Bistatic specular scattering from rough dielectric surfaces," *IEEE Transactions on Antennas and Propagation*, vol. 42, no. 2, pp. 220–231, February 1994.

[3] R. D. De Roo and F. T. Ulaby, "Authors' reply to comments on bistatic specular scattering from rough dielectric surfaces," *IEEE Transactions on Antennas and Propagation*, vol. 43, no. 2, pp. 225–226, February 1995.

4 Participating Scientific Personnel

The following people participated in the bistatic scattering program:

Faculty and Research Scientists

Professor Fawwaz T. Ulaby

Dr. Kamal Sarabandi

Graduate Students

Mr. Roger De Roo, received MS (1990), expected PhD completion in 1995.

Mr. Neil Peplinski, received MS (1993).

Mr. Andrew Zambetti, received MS (1995).

Mr. Bryan Hauck, expected MS completion in 1996.

Research Engineer

Mr. Ronald Hartikka

5 Conclusions

The bistatic scattering program has led to the development of hardware and techniques for the accurate measurement of bistatic scattering from rough surfaces. A number of important measurements has already altered our understanding of the nature of bistatic scattering, particularly in the specular direction.

By combining these measurement techniques with rough surface manufacturing techniques developed under a separate research project, a set of high quality bistatic measurements of deterministic rough surfaces is under

way. These measurements are expected to be of great value to theoreticians studying surface scattering.

A Reprints of Selected Papers

Bistatic Specular Scattering from Rough Dielectric Surfaces

Roger D. De Roo, *Student Member, IEEE,* and Fawwaz T. Ulaby, *Fellow, IEEE*

Abstract— **An experimental investigation was conducted to determine the nature of bistatic scattering from rough dielectric surfaces at 10 GHz. This paper focusses specifically on the dependence of coherent and incoherent scattered fields on surface roughness for the specular direction. The measurements, which were conducted for a smooth surface with $ks < 0.2$ (where $k = 2\pi/\lambda$ and s is the rms surface height) and for three rough surfaces with $ks = 0.5$, 1.39, and 1.94, included observations over the range of incidence angles from 20° to 65° for both horizontal and vertical polarizations. For the coherent component, the reflectivity was found to behave in accordance with the prediction of the Physical Optics model, although it was observed that the Brewster angle exhibited a small negative shift with increasing roughness. The first-order solution of Physical Optics also provided good agreement with observations for *hh*-polarized incoherent scattering coefficient, but it failed to predict the behavior of the *vv*-polarized scattering coefficient in the angular range around the Brewster angle. A second-order solution is proposed which appears to partially address the deficiency of the Physical Optics model.**

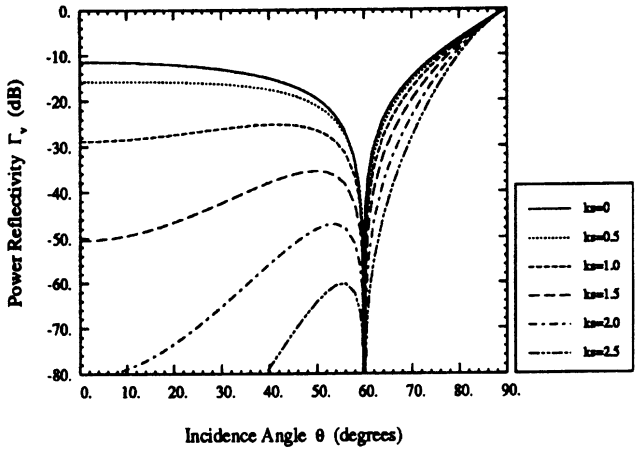

Fig. 1. Calculated coherent reflectivity for v polarization using the Physical Optics model for a Gaussian surface with ks vaired from 0 to 2.5, and $\epsilon = 3$.

I. Introduction

SCATTERING of electromagnetic fields by random rough surfaces in the backscatter direction has many uses and has been investigated extensively over the past few decades. By comparison, very few experimental investigations have been attempted to evaluate forward scattering in the specular direction. This is in part because the applications for specular scattering are not as straightforward as for backscattering. The many theoretical developments for scattering from random rough surfaces, while developed for the general bistatic case, have only been extensively used and tested for backscattering. Therefore, the usefulness and validity of these theories for specular scattering is largely unknown.

Recent developments in the modeling of terrain for radar backscattering indicate that specular scattering from a rough ground surface combined with scattering by an overstructure (such as trees or crops) can contribute significantly to the backscattering from the terrain as a whole [1]–[5]. Therefore an understanding of the nature of specular radar scattering and knowledge of the behavior of specular scattering theories are needed. Several experimental investigations were conducted at centimeter wavelengths in the 1946–1960 period to evaluate the variation of the coherent and incoherent components of the specularly reflected energy as a function of surface roughness. The results for the coherent component, which is represented by the reflection coefficient, are summarized in Beckmann and Spizzichino [6]. According to these results, the overall variation of the reflection coefficient with ks, where $k = 2\pi/\lambda$, and s is the rms height, may be explained by the coherent scattering term of the Physical Optics surface scattering model [6], [7]. The data, however, are rather lacking in several respects: (1) marginal accuracy with regard to both the measured reflected signal and the surface rms height, (2) limited dynamic range (10 dB relative to the level of the signal reflected from a perfectly smooth surface), and (3) no examination of the behavior in the angular region around the Brewster angle. Additional bistatic measurements were reported by Cosgriff *et al* [8] in 1960, but the data were not calibrated, nor were the surfaces characterized.

More recently, Ulaby *et al.* [9] measured bistatic scattering from sand and gravel surfaces at 35 GHz, and while the data were calibrated and the surfaces were characterized, no comparison to a theoretical prediction was given. In the optical regime, Saillard and Maystre [10] have measured the bistatic scattering of light from dielectric surfaces, and have observed a change in the Brewster angle as the roughness of the surface increased. Greffet [11] explained their observations using the Small Perturbation Method [12]. However, the Small Perturbation Method does not explain the observations reported in our present study: the first-order Small Perturbation Method predicts that the Brewster angle will move toward grazing as the roughness increases, while our observations indicate the opposite.

Manuscript received April 30, 1993; revised September 17, 1993. This work was supported by the Army Research Office, contract DAALO3-92-G-0269.

The authors are with The Radiation Laboratory, Department of Electrical Engineering and Computer Science, University of Michigan, Ann Arbor, MI, 48109-2122.

IEEE Log Number 9215659.

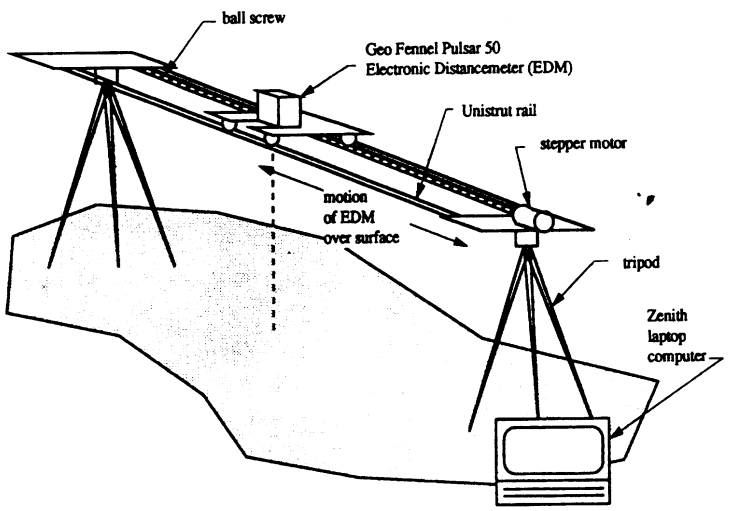

Fig. 2. Diagram of Laser Profiler.

There are three major rough surface scattering approaches which have long held the acceptance of the scientific community as valid for some ranges of surface roughness. The Geometric Optics (GO) model, the Physical Optics (PO) model, and the Small Perturbation Method (SPM) are the three theoretical approaches most commonly used at microwave frequencies for characterizing scattering from random rough surfaces [7]. While both GO and PO models rely on the Kirchhoff approach of using the tangent-plane approximation, they yield very different predictions for the scattering of waves from a rough surface. In particular, the GO model does not predict any coherent reflectivity from rough surfaces. This may appear to be an inadequacy of the GO approach; however, the GO approach is valid only for surfaces so rough that any coherent scattering would be very small anyway. The PO model, on the other hand, has a simple expression for the coherent scattering component, but the complete expression for incoherent scattering, even for single scattering, has not yet been formulated. SPM is a different approach, but its range of validity is restricted to surfaces with small rms heights and slopes. Because the ranges of validity for the GO and SPM theories are outside the range of rms heights described in this paper, comparisons to GO and SPM will not be discussed.

In this paper we will examine experimental measurements of the coherent and incoherent scattering components in the specular directions at 10 GHz for several dry sand surfaces covering a wide range of rms heights (0.5 mm to 1.4 cm). The measurements were conducted over an incidence angle range extending from 20° to 65° for both horizontal and vertical polarizations. The sand, with a relative dielectric constant of 3.0 and negligible loss factor, exhibits a null for vertical polarization at the Brewster angle of 60°. The experimental data are compared with predictions based on a revision of the Physical Optics solution that is slightly different from and more accurate than the standard form available in the literature [7].

II. Physical Optics Model—A Vector Solution

The Physical Optics approach involves integration of the Kirchhoff scattered field over the rough surface. The coherent field reflection coefficient from a surface with a Gaussian height distribution is given by [7]:

$$R_q(\theta) = R_{q0} e^{-2k^2 s^2 \cos^2\theta} \delta_{pq} \tag{1}$$

where the polarization subscripts p, q are either h or v, and $\cos\theta = -\hat{z} \cdot \hat{k}_i$. The angle θ is both the angle of incidence and reflection; coherent scattering occurs only in the specular direction from the mean surface. The reflection coefficient R_{q0} for a plane surface is given by (15) and (16) below. Fig. 1 shows $\Gamma_v(\theta) = |R_v(\theta)|^2$ for several values of ks. The Brewster angle does not change with surface roughness, but the coherent scattered power decreases very rapidly with increasing roughness.

The power in the incoherent reflected field may be given by a Taylor series in surface slope distributions. In Ulaby *et al.* [7] the Physical Optics solution is called the Scalar Approximation because slopes are ignored in the surface local coordinate system, leading to a decoupling of polarizations in the vector scattering equations. As a result, co-polarized scattering in the plane of incidence is fairly accurate, but cross-polarized scattering is zero. With the inclusion of surface slopes transverse to the plane of incidence in the vectorial solution to the Physical Optics approximation, depolarization in the plane of incidence is predicted when the Taylor series is expanded to the second order in surface slopes. The derivation is given in Appendix A. In the specular scattering direction, the first order terms are zero. The Physical Optics expression for incoherent scattering in the specular direction, which includes the zeroth and the important part of the second order terms, is given by (see last paragraph of Appendix A):

$$\sigma^0_{pq} = 2k^2 \cos^2\theta |a'_{0pq}|^2 I'_0 + 4k^4 s^4 \cos^4\theta (|a'_{lpq}|^2 + |a'_{tpq}|^2) I'_{20} \tag{2}$$

where

$$I'_0 = e^{-4k^2 s^2 \cos^2\theta} \int_0^\infty \left(e^{4k^2 s^2 \cos^2\theta \rho(\xi)} - 1\right) \xi d\xi \tag{3}$$

$$I'_{20} = \int_0^\infty \left(\frac{\partial \rho(\xi)}{\partial \xi}\right)^2 e^{-4k^2 s^2 \cos^2\theta (1-\rho(\xi))} \xi d\xi \tag{4}$$

and

$$a'_{0hh} = R_{h0} \tag{5}$$
$$a'_{lhh} = R_{h1} \tag{6}$$
$$a'_{0vv} = R_{v0} \tag{7}$$
$$a'_{lvv} = R_{v1} \tag{8}$$
$$a'_{thh} = a'_{tvv} = 0 \tag{9}$$
$$a'_{0vh} = a'_{lvh} = a'_{0hv} = a'_{lhv} = 0 \tag{10}$$
$$a'_{tvh} = (R_{h0}\cos^2\theta + R_{v0})/\sin\theta \tag{11}$$
$$a'_{thv} = -(R_{v0}\cos^2\theta + R_{h0})/\sin\theta \tag{12}$$

The a'_{0pq} terms are the zeroth-order terms (scalar approximation); the a'_{lpq} and a'_{tpq} terms are the second-order terms due to slopes longitudinal and transverse to the plane of incidence. The function $\rho(\xi)$ is the normalized correlation function of the surface, and the parameters $R_{v0}, R_{h0}, R_{v1}, R_{h1}$ are the coefficients of the (field) reflectivity local to the surface when expanded in terms of surface slopes:

$$R_h(x,y) = R_{h0} + R_{h1}Z_l(x,y) + \cdots \tag{13}$$
$$R_v(x,y) = R_{v0} + R_{v1}Z_l(x,y) + \cdots \tag{14}$$

where $Z_l(x,y)$ is the surface slope longitudinal to the direction of the incident wave at the (x,y) lateral coordinates of the surface. The zeroth-order terms are identical to the reflection coefficients for a smooth surface. In particular,

$$R_{h0} = \frac{\eta_2\cos\theta - \eta_1\cos\theta_t}{\eta_2\cos\theta + \eta_1\cos\theta_t} \tag{15}$$
$$R_{v0} = \frac{\eta_1\cos\theta - \eta_2\cos\theta_t}{\eta_1\cos\theta + \eta_2\cos\theta_t} \tag{16}$$
$$R_{h1} = \frac{\eta_2\sin\theta(1-R_{h0}) - \eta_1\frac{k_1\cos\theta}{k_2\cos\theta_t}\sin\theta_t(1+R_{h0})}{\eta_2\cos\theta + \eta_1\cos\theta_t} \tag{17}$$
$$R_{v1} = \frac{\eta_1\sin\theta(1-R_{v0}) - \eta_2\frac{k_1\cos\theta}{k_2\cos\theta_t}\sin\theta_t(1+R_{v0})}{\eta_1\cos\theta + \eta_2\cos\theta_t} \tag{18}$$

where θ_t is related to θ by Snell's Law: $k_1\sin\theta = k_2\sin\theta_t$, and $\eta = \sqrt{\mu/\epsilon}$. These first-order coefficients are different from those found in Ulaby *et al* [7] and Ulaby and Elachi [13] due to the incorporation of a more precise method for expanding the local angle of transmission.

The zeroth-order terms dominate co-polarized scattering except near the Brewster angle, where the zeroth-order terms tend toward zero. For cross-polarization, the zeroth-order terms predict no scattering for all specular angles, and therefore cross-polarized scattering is determined by the second-order terms. Unfortunately, this is still a single-scattering theory, and depolarization is very small compared to other possible sources, such as multiple scattering or volume scattering. Thus it provides a simple estimate of the minimum expected cross-polarized scattering in the specular scattering direction. The co-polarized second-order terms are all negligible except in the vicinity of the Brewster angle, where the zeroth-order terms vanish for vv polarization. The second-order terms all tend toward zero at grazing, and the cross polarized terms tend toward zero at nadir.

The fact that the Kirchhoff approximation is capable of predicting any cross-polarized single scattering in the plane of incidence is somewhat surprising. However, this is possible because the Physical Optics approximation is used in the derivation; use of the Geometric Optics approximation neglects diffraction and is incapable of predicting cross-polarized scattering. While expressions similar to, but not identical with, those described here for the higher order terms of the Physical Optics model have been presented in the past [14], and have been unsuccessful in matching experimental measurements of

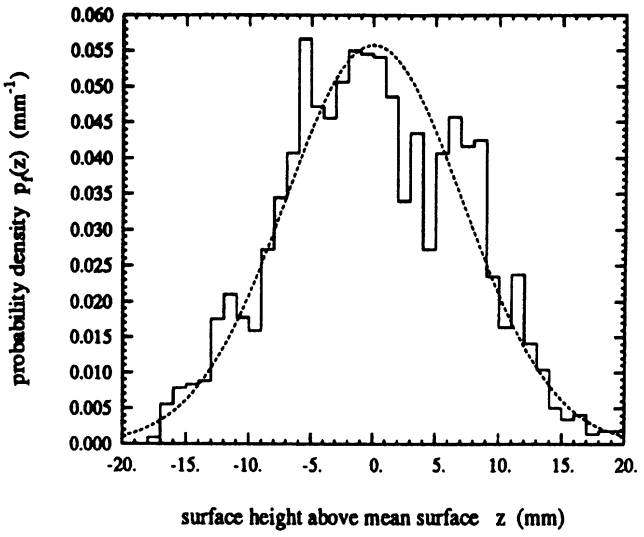

(a)

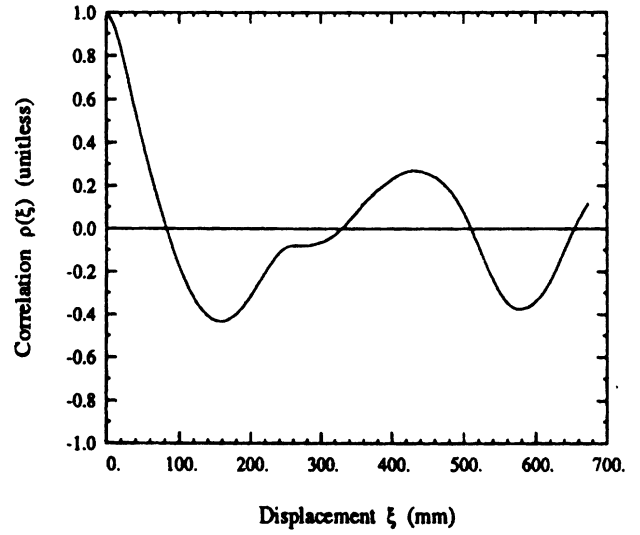

(b)

Fig. 3. Typical results of surface characterization of one of the surfaces measured in this study: (a) Histogram of measured heights for a slightly rough surface and the Gaussian probability distribution used to model it; a total of 4353 height measurements were made, from which the rms height was calculated to be $s = 6.9$ mm. (b) Measured autocorrelation function of the same surface.

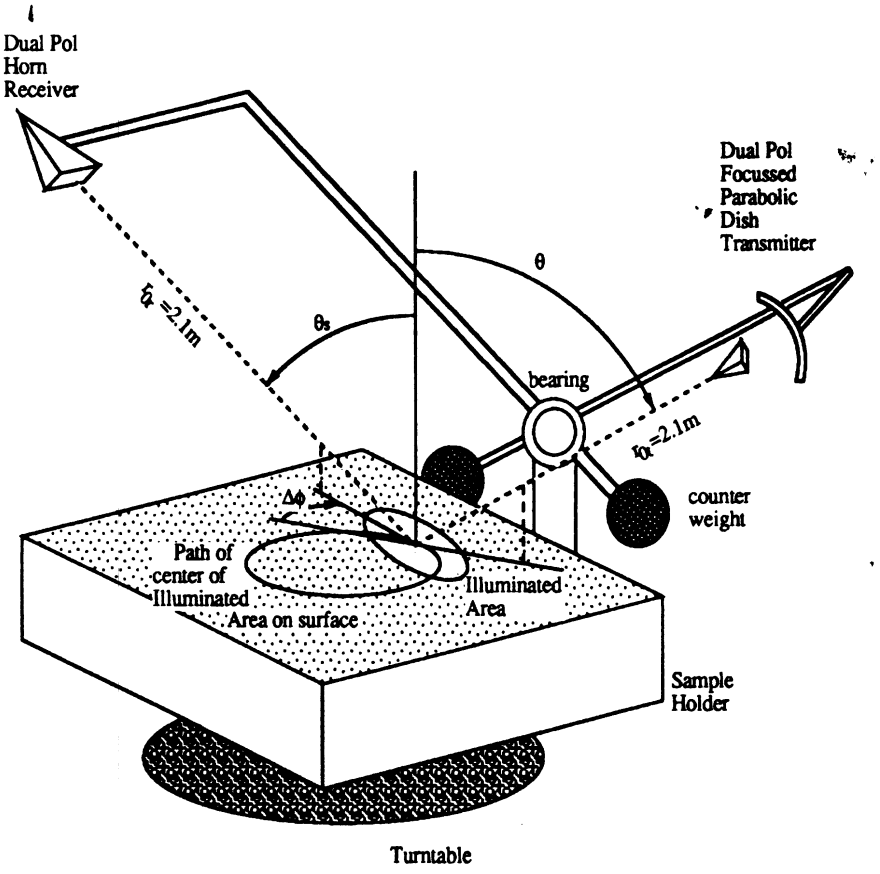

Fig. 4. Diagram of the Bistatic Facility.

the cross-polarized scattering coefficient [15], the authors are not aware of any attempt to use the higher order terms to explain scattering in the vicinity of the Brewster angle.

III. Measurement Description

A. Laser Profiler

The measurements shown in this paper are for random surfaces with varying roughness. The surfaces were characterized by a Laser Profiler, a device engineered at the University of Michigan to measure 2 meter linear or 1 meter by 1 meter square sections of surface profiles. The Profiler is shown in 2 meter linear mode in Fig. 2. Using a Pulsar 50 Electronic Distancemeter manufactured by GEO Fennel, it can measure profiles of surfaces without direct contact. The profiler has a horizontal resolution of 1 mm and a vertical resolution of 2 mm. Fig. 3(a) is an example of the height histogram generated from the profile measured for one of the surfaces, and Fig. 3(b) shows the corresponding correlation function.

B. Bistatic Facility

The configuration shown in Fig. 4 depicts the indoor bistatic radar system used for making the measurements reported in this paper. It is a stepped-frequency (8.5–10 GHz) measurement system capable of measuring the scattering matrix S of the target contained in the area or volume formed by the intersection of the transmit and receive antenna beams. Using an HP8720 vector network analyzer with an amplifier on the transmitting antenna, the system measures a complex voltage for any pair of v or h receive and transmit polarization states. With proper calibration, it is capable of measuring all four complex elements of the scattering matrix of the target surface. The hardware allows the transmitter and receiver to be located independently at any point on a hemispherical shell 2.1 m from the center of the target. In practice, however, measurements are accurate only when both antennas are within 70° of nadir.

The receive antenna is a dual-polarized horn antenna with a beamwidth of 12°, and the transmit antenna is a dual-polarized parabolic dish whose feed was designed such that the main beam of the parabolic dish is focused at a range equal to the distance to the target surface, which is held constant for all measurements. Because of the larger aperture (30 cm diameter), the transmit antenna has a narrow beam of 5°, which dictates the extent of the surface area responsible for the scattered energy. By using a focused beam antenna, we achieve a narrow-beam configuration without having to satisfy the usual far-field criterion. A baffle made of radar absorbing material was placed in the direct path between the transmitter and reciever to insure proper isolation of the two antennas.

To separate the measured signal into its coherent and incoherent components, it is necessary to measure many statistically independent samples of the random surface characterizing the target surface. This is achieved by rotating the sample holder in increments of 10°, thereby realizing 36 spatial samples per full rotation. The spatial correlation of the measured incoherent power indicates that measurements decorrelated every 15°, resulting in 24 independent samples per surface. Measurements of smooth surfaces indicate that phase coherence is maintained between independent samples.

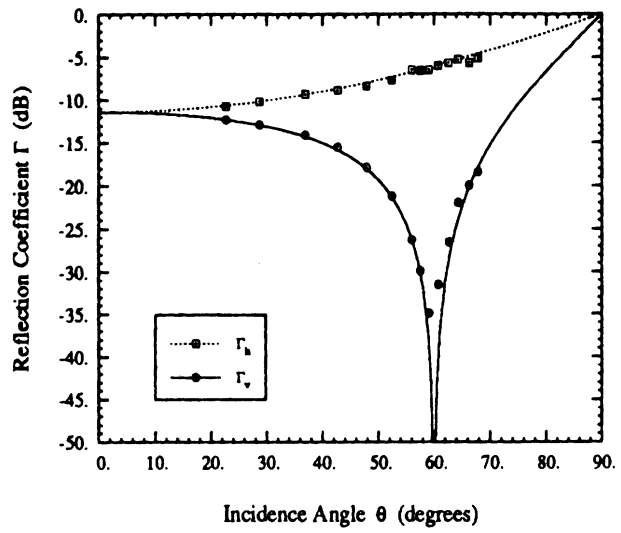

Fig. 5. Measured coherent reflectivity of a smooth surface with $\epsilon = 3.0$ and $ks < 0.2$: squares denote horizontal polarization and circles denote vertical polarization. Continuous curves are predictions based on Physical Optics. The angle of minimum reflectivity for vertical polarization is 60°.

The total path length, from transmitter to target to receiver, has a standard deviation less than 4 mm (7° at 9.25 GHz) for the set of independent samples.

C. Separation of Coherent and Incoherent Power

The Bistatic Facility measures a complex voltage V_m which is proportional to the scattered electric field for each polarization state at each spatially independent sample of the surface. Because the scattered electric field is composed of a coherent component from the mean surface and an incoherent component from the rough surface and/or volume, the measured voltage will also have a coherent and incoherent component: $V_m = V_{\text{coh}} + V_{\text{incoh}}$. These two components can be separated because the incoherent component has a zero mean: $\langle V_{\text{incoh}} \rangle = 0$. Provided a large number of independent samples are measured, the coherent power P^{coh} is proportional to the square of the complex average of the measured voltages:

$$P^{\text{coh}} = |V_{\text{coh}}|^2 = |\overline{V_m}|^2 \tag{19}$$

The incoherent power P^{incoh} is then proportional to the variance of the fluctuating component of the measured voltage:

$$P^{\text{incoh}} = \langle |V_{\text{incoh}}|^2 \rangle = \overline{|V_m - \overline{V_m}|^2} \tag{20}$$

D. Calibration

The bistatic measurement system is calibrated using a bistatic adaptation of the polarimetric backscattering calibration technique developed by Sarabandi and Ulaby [16]. For measurements corresponding to the bistatic specular configuration, a large, flat conducting plate is used as a calibration target. Further verification is obtained by measuring a conducting hemisphere placed on the calibration target. The radar cross section of the hemispherical target was calculated via Physical Optics. Calibration to date has been accurate to within 0.5 dB in magnitude and 10° in co-polarized phase difference at boresight. The system is extremely stable; while the calibration procedure is performed for each day of measurements, calibrations have been good for up to 5 days.

The bistatic facility measures E_{pq}, the p polarized field due to a q polarized transmitted field. The power in this measured field P_{pq}, is composed of a coherent and an incoherent component:

$$P_{pq} = P_{pq}^{\text{coh}} + P_{pq}^{\text{incoh}} \tag{21}$$

$$P_{pq}^{\text{coh}} = P_q^t \frac{|K_{pq}|^2}{(4\pi)^2 (r_{0r} + r_{0t})^2} \Gamma_{pq} \tag{22}$$

$$P_{pq}^{\text{incoh}} = P_q^t \frac{|K_{pq}|^2}{(4\pi)^3} \sigma_{pq}^0 \lambda^2 \int_{A_{\text{ill}}} \frac{g_p^r(x,y) g_q^t(x,y)}{r_r^2(x,y) r_t^2(x,y)} dxdy \tag{23}$$

$$= P_q^t \frac{|K_{pq}|^2}{(4\pi)^3} \sigma_{pq}^0 I_{A_{\text{ill}}\, pq} \tag{24}$$

where the coherent power reflection coefficient, and therefore the coherent power, exists only for co-polarized scattering: $P_{pq}^{\text{coh}} = \Gamma_{pq} = 0$ if $p \neq q$.

The co-polarized coherent power reflection coefficient is calculated by comparing the coherent power from a target to that from a large flat conducting plate, for which $\Gamma_{pp}^{\text{cal}} = 1$ and $\sigma_{pq}^0 = 0$. Thus,

$$\Gamma_{pp} = \frac{P_{pp}^{\text{coh}}}{P_{pp}^{\text{cal}}} \tag{25}$$

The co-polarized differential scattering coefficient is calculated by comparing the incoherent power from a target to that of the calibration power. $I_{A_{\text{ill}}pq}$ was calculated from extensive measurements of the normalized antenna patterns for both antennas, for each of the principal polarization states, over the entire main lobe of the antennas, at the boresight ranges r_{0r} and r_{0t}. Thus,

$$\sigma_{pp}^0 = \frac{4\pi}{(r_{0t} + r_{0r})^2 I_{A_{\text{ill}}\, pp}} \frac{P_{pp}^{\text{incoh}}}{P_{pp}^{\text{cal}}} \tag{26}$$

IV. Results

A. Surface Characterizations

The shape of a random rough surface is described by the surface height distribution function and the surface height correlation function. For a surface whose height is given by $z = f(x,y)$, the surface-height probability density function is given by $p_f(z)$, and is assumed to be Gaussian:

$$p_f(z) = \frac{1}{\sqrt{2\pi}s} e^{-\frac{1}{2}\frac{z^2}{s^2}} \tag{27}$$

Measurements by this and other experimenters [17], [18] indicate that this assumption is appropriate. Fig. 3(a) shows the fit between a histogram of measured surface heights and equation (27). The surface height characteristics can be specified by a single parameter, s, which is the root-mean-squared surface deviation from the mean planar surface located at $z = 0$.

The other statistical descriptor of random rough surfaces is the normalized correlation function, denoted by ρ. It describes

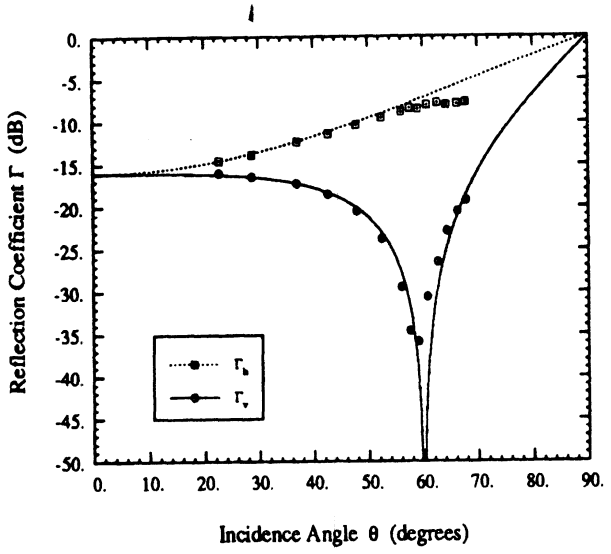

(a)

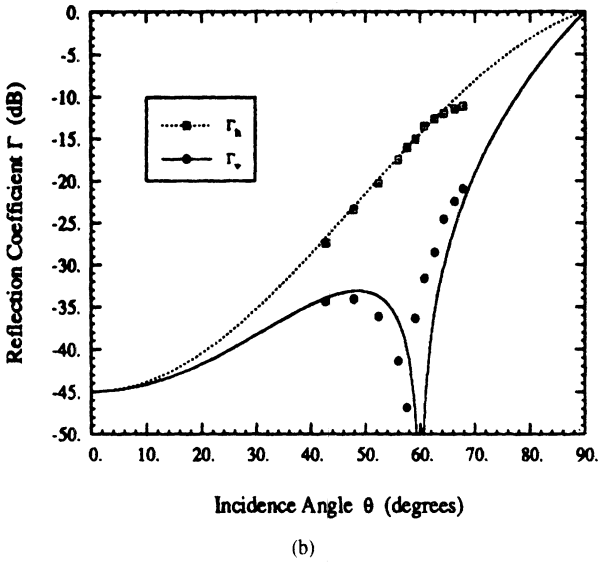

(b)

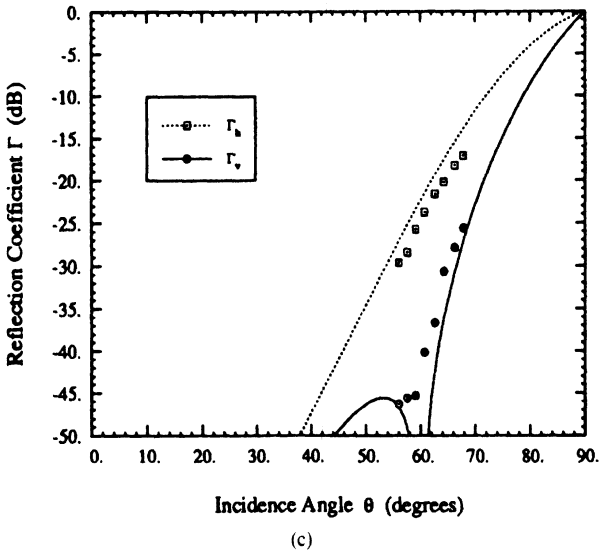

(c)

Fig. 6. Measured coherent reflectivity of three rough surfaces. Continuous curves are predictions based on Physical Optics. In all cases, the surfaces have a relative dielectric constant $\epsilon = 3.0$. (a) $ks = 0.515, kl = 5.4$. (b) $ks = 1.39, kl = 10.6$. (c) $ks = 1.94, kl = 11.8$.

the degree to which the height at one location given by $z = f(x, y)$, is correlated to the height at another location, given by $z' = f(x', y')$. For surfaces described by a stationary random process, ρ can be expressed in terms of the lateral separations $u = x - x'$ and $v = y - y'$ between the two locations on the surface. Moreover, if the surface statistics are symmetric under azimuthal rotations, the correlation function can be described by a single variable $\xi = \sqrt{u^2 + v^2}$, which specifies the absolute value of the lateral separation. Unlike the surface height distribution function, the correlation function may take on several forms for naturally occurring randomly rough surfaces. The vast majority of the literature on rough surface scattering assumes that the surface statistics are azimuthally symmetric and Gaussian, while many measurements of commonly occurring surfaces in microwave remote sensing situations indicate that an exponential correlation function may be more appropriate [19].

A correlation function for a surface with a correlation length of 52.5 mm is shown in Fig. 3(b). It was generated by averaging the individual autocorrelations of 3 linear profiles of the surface. Experimentation has shown that only 3 profile measurements averaged together are neccessary to accurately determine the correlation length and shape of this and other surfaces, but many more are needed to demonstrate that the correlation function tends toward zero beyond a few correlation lengths. For the purposes of this paper, the correlation length of a surface is that length at which the normalized correlation function is e^{-1}. As a result of the negative values of the correlation function, several of the integrals used to predict scattering characteristics ((3) and (4)) may yield values which are obviously incorrect. However, only a few surface profiles are needed to determine the shape of the correlation function within one correlation length, and if the rest of the correlation function tends towards zero, this portion of the correlation function dominates the integrals. The effect of the shape of the correlation function within one correlation length can be explored by considering several analytical forms for the correlation function.

B. Coherent Scattering

At the Brewster angle, the reflectivity for the vertical polarization is identically zero for a smooth interface between two lossless dielectric media. Whether or not it remains identically zero for a slightly rough surface is not clear. The Physical Optics approach clearly predicts that this is so; moreover, it predicts that the minimum reflectivity remains at the same incidence angle as for a smooth surface. This can be seen in Fig. 1. However, the Small Perturbation method predicts that the angle of minimum reflection for vertical polarization increases slightly with increasing roughness of the surface [11]. The fact that Physical Optics does not predict a change in angle while the Small Perturbation does is a consequence of the fact that the correction to the Fresnel coefficient is multiplicative for Physical Optics while it is additive for Small Perturbation. Additional terms in the Small Perturbation expansion may move this minimum angle back toward the smooth-surface Brewster angle.

a Fig. 5 shows measurements of the reflection coefficient for a smooth dry surface with $ks < 0.2$ (the rms height s was

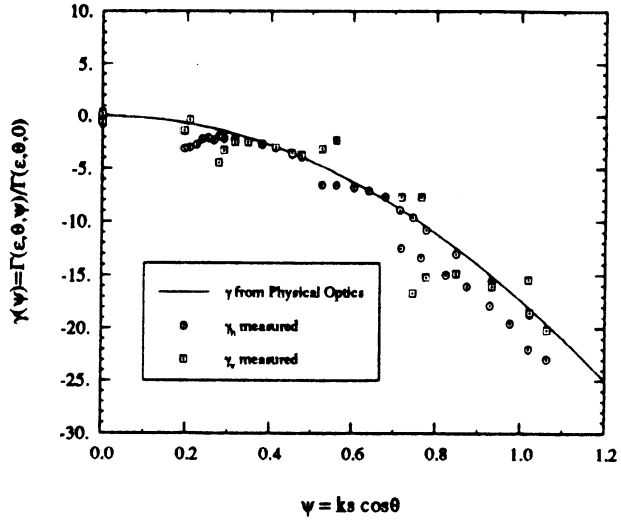

Fig. 7. The reduction of coherent scattering from a surface due to roughness. Shown is the measured coherent reflectivity of several surfaces (all with with $\epsilon' = 3$) but differing roughness parameters ψ, normalized to the reflection coefficient of a smooth surface. The angles of incidence range from 20° to 70° and the roughness ks ranges from 0 to 2. The continuous curve is the Physical Optics prediction for surfaces with Gaussian-height probability densities.

smaller than 1 mm, the measurement precision of the laser profileometer). The curves in Fig. 5 were calculated using the Fresnel reflection coefficient formulas given by (15) and (16) for a surface with a relative dielectric constant $\epsilon = 3.0 + j0$. The dielectric constant for the sand medium was measured by a dielectric probe, which gave a value of $\epsilon' = 3.0$ for the real part and a value of $\epsilon'' < 0.03$ for the imaginary part. Because $\epsilon''/\epsilon' \ll 1$ and the inclusion of ϵ'' as high as 0.05 does not significantly change the results of any of the calculations in this paper, it was ignored. The excellent agreement between the measured data and the calculated curves presented in Fig. 5 provides testimony to the measurement accuracy of the system.

Fig. 6 compares measured values of the power reflection coefficient Γ with curves calculated using Physical Optics (equation (1)) for surfaces with $ks = 0.515, 1.39$, and 1.94. Although good overall agreement is observed between theory and experimental observations, it should be noted that the location of the Brewster angle exhibits a slight shift towards decreasing angle of incidence; the Brewster angle shifts from 60° for the smooth surface shown in Fig. 5 to 58° for the surface with $ks = 1.39$ (Fig. 6(b)) and to about 56° for the surface with $ks = 1.94$ (Fig. 6(c)). The shift is toward decreasing angle of incidence, which is opposite to the direction predicted by the Small Perturbation Method.

By way of summary, Fig. 7 shows the dependence of the q-polarized normalized power reflection coefficient γ_q on the roughness parameter ψ, where

$$\gamma_q(\psi) \triangleq \frac{\Gamma_q(\epsilon,\theta,\psi)}{\Gamma_{q0}(\epsilon,\theta,0)} = \frac{|R_q|^2}{|R_{q0}|^2} \tag{28}$$

$$= e^{4\psi^2} \tag{29}$$

and $\psi = ks\cos\theta$.

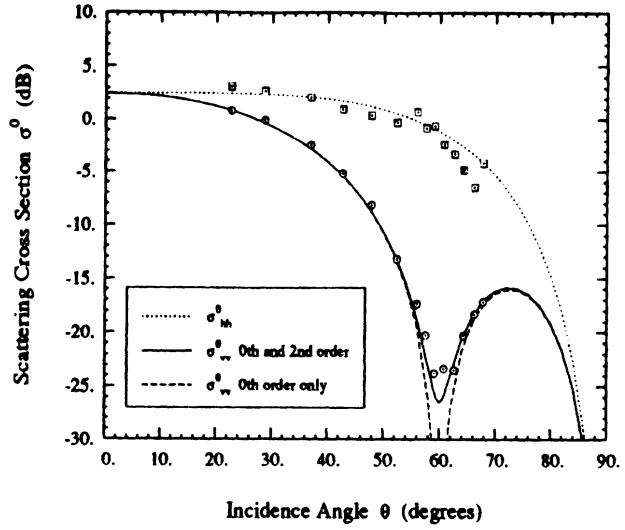

(a)

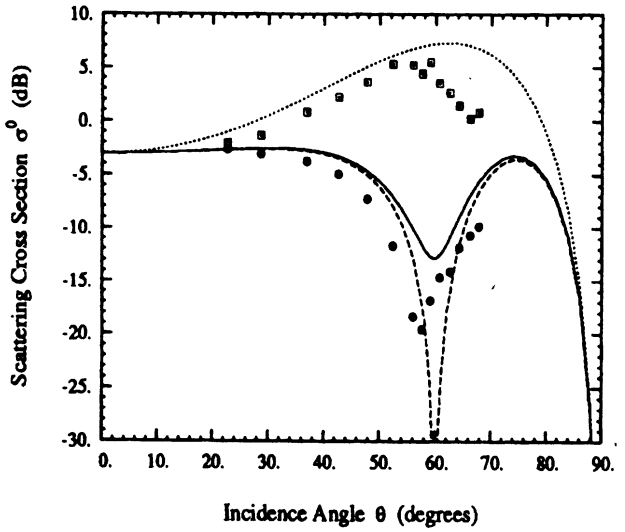

(b)

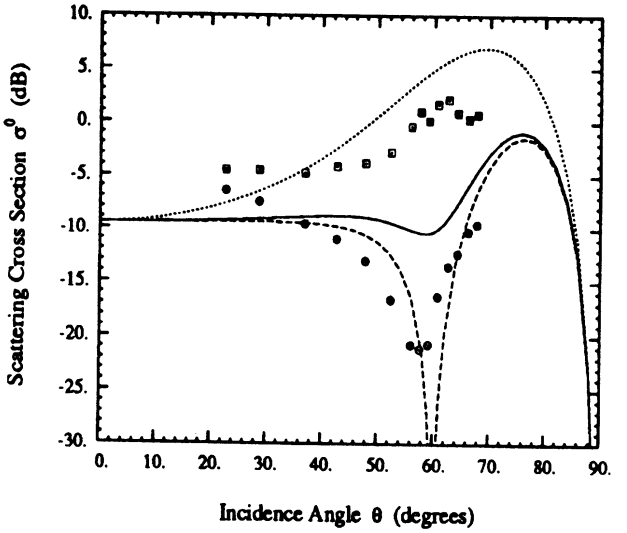

(c)

Fig. 8. Measured co-polarized specular scattering coefficient for three rough surfaces. Continuous curves are based on Physical Optics: the dashed curve corresponds to the zeroth-order term for σ^0_{vv}, the solid curve to σ^0_{vv} with both the zeroth-order and second-order terms included; the dotted curve corresponds to σ^0_{hh}. The second-order term is negligible for hh polarization. In all cases, the surfaces have a relative dielectric constant $\epsilon = 3.0$ and an exponential correlation function was used. (a) $ks = 0.515, kl = 5.4$. (b) $ks = 1.39, kl = 10.6$, (c) $ks = 1.94, kl = 11.8$.

Incoherent Scattering

As was discussed previously in Section II, the expression given by (2) for the bistatic specular scattering coefficient consists of two terms, a zeroth-order term and a second-order term, with the latter being the result of a new derivation of the Physical Optics model given in Appendix A. Fig. 8(a) shows the measured values of σ^0_{vv} and σ^0_{hh} for a slightly rough surface with $ks = 0.515$, plotted as a function of incidence angle, as well as plots for the same quantities calculated in accordance with (2). The calculated curves include a pair for the zeroth-order term alone, and a pair for the sum of the zeroth-order and second-order terms. For hh polarization, the second-order term is much smaller than the zeroth-order term, and therefore its contribution is insignificant. The same observation applies to vv polarization for angles more than 5° away from the Brewster angle, but in the vicinity of the Brewster angle, the second order term becomes the dominant contribution and it correctly predicts the level of the experimental observations.

Unfortunately, for the rougher surfaces shown in Figs. 8(b) and (c) with $ks = 1.39$ and 1.94, the model overestimates the level of σ^0, particularly for vv polarization in the vicinity of the Brewster angle. The measured data fall in between the curves calculated on the basis of the zeroth-order term alone and the curves based on both terms. Thus, despite the improvement that the proposed model provides for the slightly-rough case shown in Fig. 8(a), it is inadequate for very rough surfaces.

V. Conclusion

Several measurements of specular scattering from rough surfaces at 10 GHz are presented. They indicate that the Physical Optics predictions for coherent scattering are very good for surface roughness as large as $ks = 2.0$, with the exception that the theory does not predict a shifting of the Brewster angle by a few degrees towards nadir. A theoretical explanation of this phenomenon is unresolved. For co-polarized incoherent scattering, Physical Optics has been shown to be an adequate descriptor for a surface with $ks = 0.515$, but rapidly loses its quantitative predictive value for $ks > 1$.

Appendix A. A Vector Physical Optics Development

In Ulaby *et al.* [7], the Physical Optics solution for scattering from a dielectric rough surface is presented under the scalar approximation. This approximation leaves out many terms, some of which change the results of the calculations significantly. In particular, cross-polarized scattering is neglected in the plane of incidence under the scalar approximation. What follows is a full vector solution to the Physical Optics problem, including vector terms which are neglected via the scalar approximation and some higher order terms in the expansion of the solution with respect to surface slope, with the rest of the assumptions remaining the same as in Ulaby *et al.* [7].

The solution starts with the exact Stratton-Chu integral equation for the p-polarized scattered far field due to a q-polarized wave ($\hat{q}E_0 e^{-jk\hat{n}_i\cdot\vec{r}}$) incident upon a rough surface:

$$E^s_{pq} = \frac{-jk_s e^{-jk_s R_0}}{4\pi R_0}\hat{n}_s \times \int [(\hat{n}\times\vec{E}) - \eta_s \hat{n}_s \times (\hat{n}\times\vec{H})] \times e^{jk_s \hat{n}_s\cdot\vec{r}} dS \quad (A.1)$$

$$= \frac{-jk_s e^{-jk_s R_0}}{4\pi R_0} E_0 \int U_{pq} e^{jk_s(\hat{n}_s - \hat{n}_i)\cdot\vec{r}} dS \quad (A.2)$$

where the singly scattered fields on the surface are calculated via the tangent plane approximation and are given by:

$$\hat{n}_1 \times \vec{E} = [R_h(\hat{q}\cdot\hat{t})(\hat{n}_1\times\hat{t}) + R_v(\hat{n}_1\cdot\hat{n}_i)(\hat{q}\cdot\hat{d})\hat{t}]E_0 \quad (A.3)$$

$$\eta_1 \hat{n}_1 \times \vec{H} = [R_h(\hat{n}_1\cdot\hat{n}_i)(\hat{q}\cdot\hat{t})\hat{t} - R_v(\hat{q}\cdot\hat{d})(\hat{n}_1\times\hat{t})]E_0 \quad (A.4)$$

where $\hat{n}_i$ is the incident wave direction, $\hat{q}$ is the incident wave polarization direction, $\hat{n}_1$ is the unit normal to the surface, $\hat{t} = \hat{n}_i \times \hat{n}_1/|\hat{n}_i \times \hat{n}_1|$, and $\hat{d} = \hat{n}_i \times \hat{t}$. Also, R_v and R_h are the v- and h- polarized Fresnel Reflection coefficients local to a point on the surface. These quantities, and the appropriate vector products, are defined in Ulaby *et al.* [7]; however, the exact expressions for U_{pq} under the single scattering tangent plane approximation do not appear there and hence are given here for reference:

$$\begin{aligned} U_{hh} = \frac{1}{D_1^2 D_2}[&R_v Z_t((\sin\theta\sin\Delta\phi + Z_t^s\cos\theta + Z_t Z_l^s\sin\theta) \\ &+ (\cos\theta + Z_l\sin\theta)(\sin\theta\cos\theta_s\sin\Delta\phi \\ &+ Z_t^s\cos\theta\cos\theta_s - Z_t\sin\theta\sin\theta_s)) \\ &- R_h(\sin\theta - Z_l\cos\theta)((\cos\theta + Z_l\sin\theta) \\ &\times(\sin\theta\cos\Delta\phi - Z_l^s\cos\theta) \\ &+ (\sin\theta\cos\theta_s\cos\Delta\phi - Z_l^s\cos\theta\cos\theta_s \\ &+ Z_t Z_t^s\sin\theta\cos\theta_s - Z_l\sin\theta\sin\theta_s \\ &+ (Z_l^2 + Z_t^2)\cos\theta\sin\theta_s))] \end{aligned} \quad (A.5)$$

$$\begin{aligned} U_{vh} = \frac{1}{D_1^2 D_2}[&-R_h(\sin\theta - Z_l\cos\theta)((\sin\theta\sin\Delta\phi \\ &+ Z_t^s\cos\theta + Z_t Z_l^s\sin\theta) + (\cos\theta + Z_l\sin\theta) \\ &\times(\sin\theta\cos\theta_s\sin\Delta\phi + Z_t^s\cos\theta\cos\theta_s \\ &- Z_t\sin\theta\sin\theta_s)) \\ &- R_v Z_t((\sin\theta\cos\theta_s\cos\Delta\phi - Z_l^s\cos\theta\cos\theta_s \\ &+ Z_t Z_t^s\sin\theta\cos\theta_s - Z_l\sin\theta\sin\theta_s \\ &+ (Z_l^2 + Z_t^2)\cos\theta\sin\theta_s) \\ &+ (\cos\theta + Z_l\sin\theta) \\ &\times(\sin\theta\cos\Delta\phi - Z_l^s\cos\theta))] \end{aligned} \quad (A.6)$$

$$\begin{aligned} U_{hv} = \frac{1}{D_1^2 D_2}[&R_h Z_t((\cos\theta + Z_l\sin\theta) \\ &\times(\sin\theta\cos\Delta\phi - Z_l^s\cos\theta) \\ &+ (\sin\theta\cos\theta_s\cos\Delta\phi - Z_l^s\cos\theta\cos\theta_s \\ &+ Z_t Z_t^s\sin\theta\cos\theta_s - Z_l\sin\theta\sin\theta_s \\ &+ (Z_l^2 + Z_t^2)\cos\theta\sin\theta_s)) \\ &+ R_v(\sin\theta - Z_l\cos\theta) \\ &\times((\sin\theta\sin\Delta\phi + Z_t^s\cos\theta + Z_t Z_l^s\sin\theta) \\ &+ (\cos\theta + Z_l\sin\theta)(\sin\theta\cos\theta_s\sin\Delta\phi \\ &+ Z_t^s\cos\theta\cos\theta_s - Z_t\sin\theta\sin\theta_s))] \end{aligned} \quad (A.7)$$

$$U_{vv} = \frac{1}{D_1^2 D_2}[R_h Z_t((\cos\theta + Z_l \sin\theta)(\sin\theta\cos\theta_s \sin\Delta\phi + Z_t^s \cos\theta\cos\theta_s - Z_t \sin\theta \sin\theta_s) + (\sin\theta \sin\Delta\phi + Z_t^s \cos\theta + Z_t Z_l^s \sin\theta)) - R_v(\sin\theta - Z_l\cos\theta)((\sin\theta\cos\theta_s\cos\Delta\phi - Z_l^s\cos\theta\cos\theta_s + Z_t Z_t^s \sin\theta\cos\theta_s - Z_l\sin\theta\sin\theta_s + (Z_l^2 + Z_t^2)\cos\theta\sin\theta_s) + (\cos\theta + Z_l\sin\theta)(\sin\theta\cos\Delta\phi - Z_l^s\cos\theta))] \quad (A.8)$$

where θ and θ_s describe the incident and scattered elevation angles measured from nadir, respectively, $\Delta\phi$ describes the angular change in azimuthal direction between the incident and scattered waves, Z_l and Z_t represent the surface slopes within (longitudinal to) and transverse to the plane of incidence, respectively, Z_l^s and Z_t^s represent the surface slopes within (longitudinal to) and transverse to the plane of the scattered wave, respectively, $D_1 = |\hat{n}_i \times \hat{n}_1| = \sqrt{(\sin\theta - Z_l\cos\theta)^2 + Z_t^2}$, and $D_2 = \sqrt{1 + Z_l^2 + Z_t^2}$.

Unfortunately, the exact expressions for U are not mathematically tractable in the Stratton-Chu integral, as the surface slopes are random functions of the location on the surface. An approximate solution can be obtained by expanding U in a Taylor series in slopes and retaining only the first two terms:

$$U_{pq} = U_{pq}^{(0)} + U_{pq}^{(1)} + \cdots \quad (A.9)$$

$$= \frac{1}{D_2}(a_{0pq} + (a_{lipq}Z_l + a_{tipq}Z_t + a_{lspq}Z_l^s + a_{tspq}Z_t^s)/\sin\theta + \cdots) \quad (A.10)$$

Note that D_2 need not be expanded as it will be cancelled upon integration over $dS = D_2 dxdy$, but D_1 is Taylor expanded as follows:

$$\frac{1}{D_1^2} = \frac{1}{(\sin\theta - Z_l\cos\theta)^2 + Z_t^2} \quad (A.11)$$

$$= \frac{1}{\sin^2\theta}\left(1 - \frac{Z_t^2}{\sin^2\theta} + 2\frac{Z_l}{\tan\theta} + 3\frac{Z_l^2}{\tan^2\theta} + \cdots\right) \quad (A.12)$$

Similarly, the reflection coefficients local to the surface are also expanded in terms of slopes:

$$R_v = R_{v0} + R_{v1}Z_l + \cdots \quad (A.13)$$

$$R_h = R_{h0} + R_{h1}Z_l + \cdots \quad (A.14)$$

The reflection coefficients are not dependent on Z_l^s or Z_t^s, and depend on even powers only of Z_t. The a coefficients in the expansion of U are, for all principal linear polarization combinations, given by:

$$a_{0hh} = -R_{h0}(\cos\theta + \cos\theta_s)\cos\Delta\phi \quad (A.15)$$

$$a_{0vh} = -R_{h0}(1 + \cos\theta\cos\theta_s)\sin\Delta\phi \quad (A.16)$$

$$a_{0hv} = R_{v0}(1 + \cos\theta\cos\theta_s)\sin\Delta\phi \quad (A.17)$$

$$a_{0vv} = -R_{v0}(\cos\theta + \cos\theta_s)\cos\Delta\phi \quad (A.18)$$

$$a_{lihh} = R_{h0}(\sin\theta\sin\theta_s - (1 + \cos\theta\cos\theta_s)\cos\Delta\phi) - R_{h1}\sin\theta\cos\Delta\phi(\cos\theta + \cos\theta_s) \quad (A.19)$$

$$a_{lshh} = R_{h0}\cos\theta(\cos\theta + \cos\theta_s) \quad (A.20)$$

$$a_{tihh} = R_{v0}\sin\Delta\phi(1 + \cos\theta\cos\theta_s) \quad (A.21)$$

$$a_{tshh} = 0 \quad (A.22)$$

$$a_{livh} = -R_{h0}\sin\Delta\phi(\cos\theta + \cos\theta_s) - R_{h1}\sin\theta\sin\Delta\phi(1 + \cos\theta\cos\theta_s) \quad (A.23)$$

$$a_{lsvh} = 0 \quad (A.24)$$

$$a_{tivh} = R_{h0}\sin\theta\cos\theta\sin\theta_s - R_{v0}\cos\Delta\phi(\cos\theta + \cos\theta_s) \quad (A.25)$$

$$a_{tsvh} = -R_{h0}\cos\theta(1 + \cos\theta\cos\theta_s) \quad (A.26)$$

$$a_{lihv} = R_{v0}\sin\Delta\phi(\cos\theta + \cos\theta_s) + R_{v1}\sin\theta\sin\Delta\phi(1 + \cos\theta\cos\theta_s) \quad (A.27)$$

$$a_{lshv} = 0 \quad (A.28)$$

$$a_{tihv} = -R_{v0}\sin\theta\cos\theta\sin\theta_s + R_{h0}\cos\Delta\phi(\cos\theta + \cos\theta_s) \quad (A.29)$$

$$a_{tshv} = R_{v0}\cos\theta(1 + \cos\theta\cos\theta_s) \quad (A.30)$$

$$a_{livv} = R_{v0}(\sin\theta\sin\theta_s - (1 + \cos\theta\cos\theta_s)\cos\Delta\phi) - R_{v1}\sin\theta(\cos\theta + \cos\theta_s)\cos\Delta\phi \quad (A.31)$$

$$a_{lsvv} = R_{v0}\cos\theta(\cos\theta + \cos\theta_s) \quad (A.32)$$

$$a_{tivv} = R_{h0}\sin\Delta\phi(1 + \cos\theta\cos\theta_s) \quad (A.33)$$

$$a_{tsvv} = 0 \quad (A.34)$$

A. Differential Radar Cross Section

The elements of the covariance matrix [13] are given by:

$$\langle S_{mn}S_{pq}^*\rangle = \int\int \langle U_{mn}^* U_{pq}^* e^{jk(\hat{n}_s - \hat{n}_i)\cdot(\vec{r} - \vec{r}')}\rangle dSdS' \quad (A.35)$$

from which the differential radar cross section can be derived:

$$\sigma_{pq}^0 = \frac{k^2}{4\pi A_0}\langle S_{pq}S_{pq}^*\rangle \quad (A.36)$$

Using (A.9):

$$U_{mn}U_{pq}^* \approx U_{mn}^{(0)}U_{pq}^{(0)*} + (U_{mn}^{(0)}U_{pq}^{(1)*} + U_{mn}^{(1)}U_{pq}^{(0)*}) + U_{mn}^{(1)}U_{pq}^{(1)*} \quad (A.37)$$

and evaluating these separately, we can express σ^0 as:

$$\sigma_{pq}^0 \approx \frac{k^2}{4\pi A_0}(\langle S_{pq}S_{pq}^*\rangle_{s^0} + \langle S_{pq}S_{pq}^*\rangle_{s^1} + \langle S_{pq}S_{pq}^*\rangle_{s^2}) \quad (A.38)$$

$$\langle S_{mn}S_{pq}^*\rangle_{s^0} = \int\int \langle U_{mn}^{(0)}U_{pq}^{(0)*} e^{jk(\hat{n}_s - \hat{n}_i)\cdot(\vec{r} - \vec{r}')}\rangle dSdS' \quad (A.39)$$

$$\langle S_{mn}S_{pq}^*\rangle_{s^1} = \int\int \langle (U_{mn}^{(0)}U_{pq}^{(1)*} + U_{mn}^{(1)}U_{pq}^{(0)*}) e^{jk(\hat{n}_s - \hat{n}_i)\cdot(\vec{r} - \vec{r}')}\rangle dSdS' \quad (A.40)$$

$$\langle S_{mn}S_{pq}^*\rangle_{s^2} = \int\int \langle U_{mn}^{(1)}U_{pq}^{(1)*} e^{jk(\hat{n}_s - \hat{n}_i)\cdot(\vec{r} - \vec{r}')}\rangle dSdS' \quad (A.41)$$

To obtain explicit expressions for σ^0_{pq}, the following relations will be used [7]:

$$\langle e^{jq_z(z-z')}\rangle = e^{-q_z^2 s^2(1-\rho(\xi))} \quad \text{(A.42)}$$

$$\langle Z_x e^{jq_z(z-z')}\rangle = \langle Z'_x e^{jq_z(z-z')}\rangle = -jq_z s^2 \cos\alpha \frac{\partial\rho(\xi)}{\partial\xi} e^{-q_z^2 s^2(1-\rho(\xi))} \quad \text{(A.43)}$$

$$\langle Z_y e^{jq_z(z-z')}\rangle = \langle Z'_y e^{jq_z(z-z')}\rangle = -jq_z s^2 \sin\alpha \frac{\partial\rho(\xi)}{\partial\xi} e^{-q_z^2 s^2(1-\rho(\xi))} \quad \text{(A.44)}$$

$$\langle Z_x Z'_x e^{jq_z(z-z')}\rangle = -\cos^2\alpha \left(q_z s^2 \frac{\partial\rho(\xi)}{\partial\xi}\right)^2 e^{-q_z^2 s^2(1-\rho(\xi))} \quad \text{(A.45)}$$

$$\langle Z_y Z'_y e^{jq_z(z-z')}\rangle = -\sin^2\alpha \left(q_z s^2 \frac{\partial\rho(\xi)}{\partial\xi}\right)^2 e^{-q_z^2 s^2(1-\rho(\xi))} \quad \text{(A.46)}$$

$$\langle Z_x Z'_y e^{jq_z(z-z')}\rangle = \langle Z_y Z'_x e^{jq_z(z-z')}\rangle = -\sin\alpha\cos\alpha \times \left(q_z s^2 \frac{\partial\rho(\xi)}{\partial\xi}\right)^2 e^{-q_z^2 s^2(1-\rho(\xi))} \quad \text{(A.47)}$$

as well as the following Bessel function integral identity:

$$\int_{2\pi} \cos(n\alpha+\beta) e^{jx\cos\alpha} d\alpha = 2\pi j^n \cos\beta J_n(x) \quad \text{(A.48)}$$

where $q_z = k(\cos\theta + \cos\theta_s)$, s is the rms height, (ξ,α) are the polar coordinates of the difference between the unprimed and primed surface locations, and $\rho(\xi)$ is the normalized surface height correlation function.

B. Zeroth Order Term

The analysis of the zeroth order term is straightforward and yields the traditional coefficients for Physical Optics:

$$\frac{k^2}{4\pi A_0}\langle S_{mn}S^*_{pq}\rangle_{s^0} = \frac{1}{4\pi}k^2 a_{0mn}a^*_{0pq} I_0 \frac{1}{4\pi}k^2 a_{0mn}a^*_{0pq} I_0 \quad \text{(A.49)}$$

where

$$I_0 = 2\pi e^{-q_z^2 s^2}\int_0^\infty [e^{q_z^2 s^2 \rho(\xi)} - 1] J_0(q_t\xi)\xi d\xi \quad \text{(A.50)}$$

$$q_t = k\sqrt{\sin^2\theta + \sin^2\theta_s - 2\sin\theta\sin\theta_s\cos\Delta\phi} \quad \text{(A.51)}$$

This term represents the expected power in a particular direction due to the correlation of the height of the surface at one point to the height at another point. This term is the largest contribution to σ^0.

C. First Order Term

The first order term in Ulaby *et al.* [7] is that of the scalar approximation. Below is the full vector solution under the tangent plane approximation:

$$\frac{k^2}{4\pi A_0}\langle S_{mn}S^*_{pq}\rangle_{s^1} = \frac{-k^2}{4\pi q_z \sin\theta}[(a_{0mn}a^*_{lipq} + a_{limn}a^*_{0pq})q_{li} + (a_{0mn}a^*_{lspq} + a_{lsmn}a^*_{0pq})q_{ls} + (a_{0mn}a^*_{tipq} + a_{timn}a^*_{0pq})q_{ti} + (a_{0mn}a^*_{tspq} + a_{tsmn}a^*_{0pq})q_{ts}]I_0 \quad \text{(A.52)}$$

where

$$q_{li} = k(\sin\theta_s\cos\Delta\phi - \sin\theta) \quad \text{(A.53)}$$

$$q_{ti} = k\sin\theta_s\sin\Delta\phi \quad \text{(A.54)}$$

$$q_{ls} = k(\sin\theta_s - \sin\theta\cos\Delta\phi) \quad \text{(A.55)}$$

$$q_{ts} = k\sin\theta\sin\Delta\phi \quad \text{(A.56)}$$

This term represents the expected power in a particular direction due to the correlation of height of the surface at one point to the slope at another point. This term is negligible for scattering in the plane of incidence.

D. Second Order Term

The cross-slope term does not appear in Ulaby *et al* [7], but is nonetheless an analytic term. It is given by:

$$\begin{aligned}\frac{k^2}{4\pi A_0}&\langle S_{mn}S^*_{pq}\rangle_{s^2} = \frac{k^2 q_z^2 s^4}{4\sin^2\theta}\{[a_{limn}a^*_{lipq} + a_{lsmn}a^*_{lspq} \\ &+ a_{timn}a^*_{tipq} + a_{tsmn}a^*_{tspq} \\ &+ ((a_{lsmn}a^*_{tipq} + a_{timn}a^*_{lspq}) \\ &- (a_{limn}a^*_{tspq} + a_{tsmn}a^*_{lipq}))\sin\Delta\phi \\ &+ ((a_{limn}a^*_{lspq} + a_{lsmn}a^*_{lipq}) \\ &+ (a_{timn}a^*_{tspq} + a_{tsmn}a^*_{tipq}))\cos\Delta\phi]I_{20} \\ &- [(a_{limn}a^*_{lipq} - a_{timn}a^*_{tipq})(q_{li}^2 - q_{ti}^2) \\ &+ (a_{lsmn}a^*_{lspq} - a_{tsmn}a^*_{tspq})(q_{ls}^2 - q_{ts}^2) \\ &- (a_{limn}a^*_{tipq} + a_{timn}a^*_{lipq})q_{ti}q_{li} \\ &- (a_{lsmn}a^*_{tspq} + a_{tsmn}a^*_{lspq})q_{ts}q_{ls} \\ &+ ((a_{limn}a^*_{tspq} + a_{tsmn}a^*_{lipq}) \\ &+ (a_{lsmn}a^*_{tipq} + a_{timn}a^*_{lspq}))(q_{ti}q_{ls} + q_{li}q_{ts}) \\ &+ ((a_{limn}a^*_{lspq} + a_{lsmn}a^*_{lipq}) \\ &- (a_{timn}a^*_{tspq} + a_{tsmn}a^*_{tipq})) \\ &\times (q_{li}q_{ls} + q_{ti}q_{ts})]I_{22}\}\end{aligned} \quad \text{(A.57)}$$

where

$$I_{20} = \int_0^\infty \left(\frac{\partial\rho(\xi)}{\partial\xi}\right)^2 J_0(q_t\xi) e^{-q_z^2 s^2(1-\rho(\xi))}\xi d\xi \quad \text{(A.58)}$$

$$I_{22} = \int_0^\infty \left(\frac{\partial\rho(\xi)}{\partial\xi}\right)^2 \frac{J_2(q_t\xi)}{q_t^2} e^{-q_z^2 s^2(1-\rho(\xi))}\xi d\xi \quad \text{(A.59)}$$

This term represents the expected power in a particular direction due to the correlation of slope of the surface at one point to the slope at another point. This term is significant for cross polarization in the plane of incidence, and when the angle of incidence is near the Brewster angle for the mean surface.

E. Evaluation of the I Integrals for Common Correlation Functions

The remaining integrals can be further simplified if we assume a form for the correlation function $\rho(\xi)$. In particular, if it is Gaussian, i.e., $\rho(\xi) = e^{-\xi^2/l^2}$, then

$$I_0 = \pi l^2 e^{-q_z^2 s^2} \sum_{i=1}^{\infty} \frac{(q_z s)^{2i}}{i!i} e^{-\frac{q_t^2 l^2}{4i}} \tag{A.60}$$

$$I_{20} = 2e^{-q_z^2 s^2} \sum_{i=1}^{\infty} \frac{i(q_z s)^{2(i-1)}}{(i+1)!(i+1)} e^{-\frac{q_t^2 l^2}{4(i+1)}} \left(1 - \frac{q_t^2 l^2}{4(i+1)}\right) \tag{A.61}$$

$$I_{22} = \frac{1}{2} l^2 e^{-q_z^2 s^2} \sum_{i=1}^{\infty} \frac{i(q_z s)^{2(i-1)}}{(i+1)!(i+1)^2} e^{-\frac{q_t^2 l^2}{4(i+1)}} \tag{A.62}$$

or, if the correlation function is exponential, i.e., $\rho(\xi) = e^{-\xi/l}$, then

$$I_0 = 2\pi l^2 e^{-q_z^2 s^2} \sum_{i=1}^{\infty} \frac{(q_z s)^{2i}}{(i-1)!(i^2 + q_t^2 l^2)^{\frac{3}{2}}} \tag{A.63}$$

$$I_{20} = e^{-q_z^2 s^2} \sum_{i=1}^{\infty} \frac{(i+1)(q_z s)^{2(i-1)}}{(i-1)!(i^2 + q_t^2 l^2)^{\frac{3}{2}}} \tag{A.64}$$

$$I_{22} = 2l^2 e^{-q_z^2 s^2} \sum_{i=1}^{\infty} \frac{(q_z s)^{2(i-1)} \left(\sqrt{(i+1)^2 + q_t^2 l^2} - (i+1)\right)}{(i-1)!((i+1)^2 + q_t^2 l^2)^{\frac{3}{2}} q_t^2 l^2} \times \left(1 - (i+1)\frac{\sqrt{(i+1)^2 + q_t^2 l^2} - (i+1)}{2q_t^2 l^2}\right) \tag{A.65}$$

F. Special Case: Forward Scattering in the Specular Direction

For forward scattering in the specular direction, $\theta_s \to \theta, \Delta\phi \to 0$, and $q_t \to 0$, and the general expressions above simplify considerably:

$$\frac{k^2}{4\pi A_0} \langle S_{mn} S_{pq}^* \rangle_{s^0} = \frac{1}{4\pi} k^2 a_{0mn} a_{0pq}^* I_0 \tag{A.66}$$

$$\frac{k^2}{4\pi A_0} \langle S_{mn} S_{pq}^* \rangle_{s^1} = 0 \tag{A.67}$$

$$\frac{k^2}{4\pi A_0} \langle S_{mn} S_{pq}^* \rangle_{s^2} = \frac{k^4 s^4}{\tan^2\theta} [(a_{limn} + a_{lsmn})(a_{lipq}^* + a_{lspq}^*) + (a_{timn} + a_{tsmn})(a_{tipq}^* + a_{tspq}^*)] I_{20} \tag{A.68}$$

where

$$a_{0hh} = -2R_{h0}\cos\theta \tag{A.69}$$

$$a_{0vh} = a_{0hv} = 0 \tag{A.70}$$

$$a_{0vv} = -2R_{v0}\cos\theta \tag{A.71}$$

$$a_{livv} + a_{lsvv} = -2R_{v1}\sin\theta\cos\theta \tag{A.72}$$

$$a_{livh} + a_{lsvh} = a_{lihv} + a_{lshv} = 0 \tag{A.73}$$

$$a_{lihh} + a_{lshh} = -2R_{h1}\sin\theta\cos\theta \tag{A.74}$$

$$a_{tivh} + a_{tsvh} = -2(R_{h0}\cos^2\theta + R_{v0})\cos\theta \tag{A.75}$$

$$a_{tihv} + a_{tshv} = 2(R_{v0}\cos^2\theta + R_{h0})\cos\theta \tag{A.76}$$

$$a_{tivv} + a_{tsvv} = a_{tihh} + a_{tshh} = 0 \tag{A.77}$$

$$I_0 = 2\pi e^{-q_z^2 s^2} \int_0^{\infty} [e^{q_z^2 s^2 \rho(\xi)} - 1]\xi d\xi \tag{A.78}$$

$$I_{20} = \int_0^{\infty} \left(\frac{\partial\rho(\xi)}{\partial\xi}\right)^2 e^{-q_z^2 s^2 (1-\rho(\xi))} \xi d\xi \tag{A.79}$$

For the principal linear polarizations $pq = hh, hv, vh, vv$, the incoherent specular scattering coefficient can be obtained by setting $mn = pq$ in (A.66) and (A.68) and the resultant expressions in (A.38) This process leads to the expression given in 920.

REFERENCES

[1] K. C. McDonald, M. C. Dobson and F. T. Ulaby, "Using MIMICS to model L-band multi-angle and multi-temporal backscatter from a walnut orchard," *IEEE Transactions on Geoscience and Remote Sensing*, vol. 28, no. 3, pp. 477–491, May 1990.

[2] K. C. McDonald, M. C. Dobson and F. T. Ulaby, "Modeling multi-frequency diurnal backscatter from a walnut orchard," *IEEE Transactions on Geoscience and Remote Sensing*, vol. 29, no. 6, pp. 852–863, 1991.

[3] K. C. McDonald, *Modeling Microwave Backscatter from Tree Canopies*, PhD dissertation, University of Michigan, Ann Arbor, 1991.

[4] F. T. Ulaby, K. Sarabandi, K. C. McDonald, M. Whitt and M. C. Dobson, "Michigan Microwave Conopy Scattering Model," *International Journal of Remote Sensing*, vol. 11, no. 7, pp. 1223–1253, 1990.

[5] M. Whitt, *Microwave Scattering from Periodic Row-Structured Vegetation*, PhD dissertation, University of Michigan, Ann Arbor, 1991.

[6] P. Beckmann and A. Spizzichino, *The Scattering of Electromagnetic Waves from Rough Surfaces*, Pergamon Press, Oxford, 1963.

[7] F. T. Ulaby, R. K. Moore and A. K. Fung, *Microwave Remote Sensing: Active and Passive*, volume 2, Addison-Wesley, Reading, Massachusetts, 1982.

[8] R. L. Cosgriff, W. H. Peake and R. C. Taylor, "Terrain scattering properties for sensor system design," *Technical Report* 181, Ohio State University, 1960.

[9] F. T. Ulaby, T. F. Haddock and M. E. Coluzzi, "Millimeter-wave bistatic radar measurements of sand and gravel," in *Digest, IEEE International Geoscience and Remote Sensing Symposium* (IGARSS'87), pp. 281–286, Ann Arbor, MI, May 1987.

[10] M. Saillard and D. Maystre, "Scattering from metallic and dielectric rough surfaces," *Journal of the Optical Society of America A*, vol. 7, no. 6, pp. 982–990, June 1990.

[11] J.-J. Greffet, "Theoretical model of the shift of the Brewster angle on a rough surface," *Optics Letters*, vol. 17, no. 4, pp. 238–240, February 1992.

[12] S. O. Rice, "Reflection of electromagnetic waves from slightly rough surfaces," *Communications in Pure and Applied Mathematics*, vol. 4, pp. 351–378, 1951.

[13] F. T. Ulaby and E. C. Elachi, *Radar Polarimetry for Geoscience Applications*, Artech House, Norwood, Massachusetts, 1990.

[14] J. C. Leader, "Bidirectional scattering of electromagnetic waves from rough surfaces," *Journal of Applied Physics*, vol. 42, no. 12, pp. 4808–4816, November 1971.

[15] J. C. Leader and W. A. J. Dalton, "Bidirectional scattering of electromagnetic waves from the volume of dielectric materials," *Journal of Applied Physics*, vol. 43, no. 7, pp. 3080–3090, July 1972.

[16] K. Sarabandi and F. T. Ulaby, "A convenient technique for polarimetric calibration of single-antenna radar systems," *IEEE Transactions on Geoscience and Remote Sensing*, vol. 28, no. 6, pp. 1022–1033, November 1990.

[17] K. A. O'Donnell and E. R. Mendez, "Experimental study of scattering from characterized random surfaces," *Journal of the Optical Society of America*, vol. 4, no. 7, pp. 1194–1205, July 1987.

[18] E. R. Mendez and K. A. O'Donnell, "Observation of depolarization and backscattering enhancement in light scattering from Gaussian rendom surfaces," *Optics Communications*, vol. 61, no. 2, pp. 91–95, January 1987.

[19] Y. Oh, K. Sarabandi and F. T. Ulaby, "An empirical model and an inversion technique for radar scattering from bare soil surfaces," *IEEE Transactions on Geoscience and Remote Sensing*, vol. 30, no. 2, pp. 370–381, March 1992.

Roger D. De Roo (S'88) was born in Ridgewood, NJ, on February 29, 1964. He received the B.S. degree in letters and engineering from Calvin College, Grand Rapids, MI, in 1986, and the B.S.E. and M.S.E. degrees from the University of Michigan, Ann Arbor, both in electrical engineering, in 1986 and 1989, respectively.

He is currently a candidate for the Ph.D. degree at the University of Michigan. His research interests include modeling and measurement of bistatic scattering of electromagnetic waves from rough surfaces ınd modeling electromagnetic scattering from vegetation.

Fawwaz T. Ulaby (M'68–SM'74–F'80) received the B.S. degree in physics from the American University of Beirut, Lebanon, in 1964 and the M.S.E.E. and Ph.D. degrees in electrical engineering from the University of Texas, Austin, TX, in 1966 and 1968, respectively.

Dr. Ulaby is the Williams Professor of Electrical Engineering and Computer Science and the Director of the NASA Center for Space Terahertz Technology at the University of Michigan, Ann Arbor. His current interests include microwave and millimeter-wave remote sensing, radar systems, and radio wave propagation. He is the recipient of numerous awards, including the Eta Kappa Nu Association C. Holmes MacDonald Award as "An Outstanding Electrical Engineering Professor in the United States of America for 1975," the IEEE Geoscience and Remote Sensing Distinguished Achievement Award (1983), the IEEE Centennial Medal (1984), the American Society of Photogrammetry's Presidential Citation for Meritorious Service (1984), the Kuwait Prize in applied science (1986), the NASA Group Achievement Award (1990), and the University of Michigan Distinguished Faculty Achievement Award (1991).

Professor Ulaby served as president of the IEEE Geoscience and Remote Sensing Society (1980–1982), as Executive Editor of its *Transactions* (1983–1985), and as General Chairman of several international symposia. he is a member of URSI Commission F and served on several scientific boards and professional committees.

Comments on "Bistatic Specular Scattering from Rough Dielectric Surfaces"

Jean-Jacques Greffet

Abstract— **In a recent paper[1], De Roo and Ulaby have reported experimental results for the coherent bistatic scattering by a random rough surface. They have found a negative shift of the Brewster angle. We show that their results are in agreement with all the previously reported theoretical and numerical calculations.**

In a recent paper,[1] De Roo and Ulaby have presented a comparison between experimental data and the Kirchhoff specular bistatic scattering. They have shown that the simple Kirchhoff result agrees with the data, except near the Brewster angle θ_B. In the vicinity of θ_B, the authors have found that the zero becomes a minimum and that there is a shift $\Delta\theta$ of this minimum. If we define the shift as $\Delta\theta = \theta_{\min} - \theta_B$, the shift is negative, which means that the minimum moves toward the normal of the surface. I would like to correct two statements that appear in the paper by De Roo and Ulaby in the discussion of this point.

The shift was first observed on numerical simulations (but not experimentally, as stated in the paper) for one-dimensional random rough surfaces by Saillard and Maystre [1]. Hence, the paper by De Roo and Ulaby is the first experimental report on this effect for random rough surfaces.

The second point deals with the sign of the shift of the Brewster angle θ_B. De Roo and Ulaby have observed that the shift is always negative. This result was reported in [1]. In a later paper [2], I have proposed a simple model based on a perturbation model to explain the physical mechanism responsible of this shift. It predicts a negative shift. Saillard has published a slightly different approach which also yields the same result [3]. The above references deal with one-dimensional surfaces. In a recent paper [4], we have derived a perturbative expression for the coherent reflected field for a two-dimensional surface. This new expression also yields a negative shift. Therefore, the observed shifts reported by De Roo and Ulaby agree with all the previous works in contrast with their statement in their Introduction and their Conclusion.

Let us briefly describe a simple mechanism in order to get some physical insight on this effect. Using a perturbative approach, the amplitude $A(\theta)$ of the coherent field can be written as the sum of two contributions: the zero-order field (amplitude $A^{(0)}$) which is given by Fresnel reflection factor, and the second-order contribution (amplitude $A^{(2)}$) due to the roughness

$$A(\theta) = A^{(0)}(\theta) + A^{(2)}(\theta).$$

It can be shown that the imaginary part of $A^{(2)}$ is much smaller than its real part. Thus, we may assume as a first approximation that both $A^{(0)}(\theta)$ and $A^{(2)}(\theta)$ are real. The minima are produced when the two contributions have the same modulus and opposite sign. This happens for θ smaller than θ_B.

Finally, I would like to mention that the same mechanism holds for the shift of the total absorption observed in the numerical calculations reported by Garcia and Stoll [5]. In this case, the reflection minima are due to the total absorption of light by a sinusoidal grating when a surface plasmon is resonantly excited. In their calculations, Garcia and Stoll have added a small random component to the sinusoidal surface. They have found that the minima for the reflected field are shifted. Again, this effect can be understood on the basis of an interference between the specularly reflected field $A^{(0)}(\theta)$ by the nonperturbed grating and the coherent amplitude $A^{(2)}(\theta)$ due to the roughness.

References

[1] M. Saillard and D. Maystre, "Scattering from metallic and dielectric surfaces," *J. Opt. Soc. Amer., A* vol. 7, pp. 982–990, 1990.
[2] J. J. Greffet, "Theoretical model of the shift of the Brewster angle on a rough surface," *Opt. Lett.*, vol. 17, pp. 238–240, 1992.
[3] M. Saillard, "A characterization tool for dielectric rough surfaces: Brewster's phenomenon," *Waves Random Media*, vol. 2, pp. 67–79, 1992.
[4] C. Baylard, J.-J. Greffet, and A. A. Maradudin, "Coherent reflection factor of a random rough surface. Applications," *J. Opt. Soc. Amer., A*, vol. 10, pp. 2637–2647, 1993.
[5] N. Garcia and E. Stoll, "Monte-Carlo calculation for electromagnetic wave scattering from random rough surfaces," *Phys. Rev. Lett.*, vol. 52, pp. 1798–1801, 1984.

Manuscript received June 6, 1994.

The author is with the Laboratoire d'Energétique Moléculaire, Macroscopique Combustion, CNRS, Ecole Centrale Paris F-92295 Châtenay-Malabry Cedex, France.

IEEE Log Number 9408253.

[1] R. D. De Roo and F. T. Ulaby, *IEEE Trans. Antennas Propagat.*, vol. 42, pp. 220–231, 1994.

Comments on "Bistatic Specular Scattering from Rough Dielectric Surfaces"

Marc Saillard

Recently, the above paper[1] has been published describing an experimental work on scattering by dielectric rough surfaces, and investigating the shift of the Brewster angle when a plane interface becomes randomly modulated. I have some comments about this aspect of the paper.

As mentioned by the authors,[1] the numerical evidence of the phenomenon has been given in [1], where rigorous computations have shown that the minimum of the reflected intensity is shifted toward lower incidence angles. This conclusion, concerning one-dimensional surfaces under p polarization, is in agreement with the aforementioned experimental work.[1] Later, with the help of the perturbation methods, a more detailed study has been achieved by several authors for both

Manuscript received June 13, 1994.

M. Saillard is with the Faculte des Science de St. Jerome, Optique Electromagnetique, 13397 Marseille Cedex 20, France.

IEEE Log Number 9408251.

[1] R. D. De Roo and F. T. Ulaby, *IEEE Trans. Antennas Propagat.*, vol. 42, pp. 220–231, 1994.

one-dimensional surfaces [2]–[4] and two dimensional surfaces [5]. The main point is that although the theories are not the same, they all lead to the same conclusion and confirm the previous results. Therefore, I am very surprised to read in the introduction[1] that a shift toward grazing angles was predicted.

Section B[1] also requires some comments. It is suggested that not enough terms of the expansion are taken into account in the perturbation method. I recall that in [3] the reflection coefficient is expanded up to second order (the first order does not concern coherent scattering) and that, within the Rayleigh hypothesis, the coefficients are rigorously calculated. Even though we do not know accurately what is the radius of convergence of such an expansion, a range of rms heights exists where the theory gives accurate results. In addition, a confrontation with rigorous computations is also achieved in [3] and the results agree quite well when the rms height is less than a tenth of the incident wavelength, thus for significant shifts of the Brewster angle.

The perturbation theory, as well as rigorous computations, also predicts that the minimum of the reflectivity is no longer rigorously zero.

Fig. 6(a)[1] deals with parameters within the domain of validity of perturbation methods, thus the experimental results could be compared with theoretical ones, while in Fig. 6(b) the rms height probably exceeds the possibilities of these theories.

I would like to add one more comment. On p. 1, the authors write that Greffet and Saillard "state that the small perturbation method predicts just the opposite..." but (later) they refer to [1], which only contains rigorous results from an integral theory. The results from the perturbation theory are given in [3]. This remark permits me to recall that the shift of the Brewster angle has also been investigated with the help of a rigorous theory which suffers no limitation with respect to the geometrical parameters of the surface. In [3] a comparison of rigorous computations with data from the perturbation method is given, and shows a very good agreement for shallow surfaces.

In the Author's Reply, it seems that two kinds of perturbation theories exist; those which give a shift toward nadir and those which lead to the opposite. According to me, it is more important to notice that the perturbation theories which, in the frame of the Rayleigh hypothesis, calculate rigorously the coefficients of the expansion of the reflection coefficient, lead to a good quantitative agreement with both rigorous computations and measurements (as shown in Fig. 1 of the reply).

As a conclusion, I suggest modifying a few sentences,[1] related to the shift of the Brewster angle: the last sentence of p. 220, the end of the first paragraph of section B, p. 225, the last comment on Fig. 6, p. 226, and the concerned sentence of the conclusion.

References

[1] M. Saillard and D. Maystre, "Scattering from metallic and dielectric rough surfaces," *JOSA A*, vol. 7, no. 6, pp. 982–990, 1990.

[2] J. J. Greffet, "Theoretical model of the shift of the Brewster angle on a rough surface," *Optics Letters*, vol. 17, pp. 238–240, 1992.

[3] M. Saillard, "A characterization tool for dielectric random rough surfaces: Brewster's phenomenon," *Waves in Random Media*, vol. 2, pp. 67–79, 1992.

[4] A. A. Maradudin, R. E. Luna, and E. R. Mendez, "The Brewster effect for a one-dimensional random surface," *Waves in Random Media*, vol. 3, pp. 51–60, 1993.

[5] C. Baylard, J. J. Greffet, and A. A. Maradudin, "Coherent reflection factor of a random rough surface: applications," *JOSA A*, vol. 10, pp. 2637–2647, 1993.

Authors' Reply

Roger D. De Roo and Fawwaz T. Ulaby

The comments contributed independently by Greffet and Saillard are basically the same and may be distilled down to two issues:

a) Their theoretical and numerical calculations predict that the Brewster angle shifts in the direction of normal incidence (negative shift) as the surface roughness increases, and our experimental results indeed support their prediction. We clearly have no disagreement with this comment and are in fact pleased that our data confirms their theory.

b) In our paper [1], we stated that "the small perturbation method does not explain the observations reported in our present study: the first-order small perturbation method predicts that the Brewster angle will move toward grazing as the roughness increases, while our observations indicate the opposite." This statement is incorrect and both Greffet and Saillard take exception to it. The small perturbation method (SPM) predicts that the Brewster angle is toward the nadir.

Our statements regarding SPM were based on the expressions given in Tsang *et al.* [2]. Unfortunately, the published expression for the SPM vertically polarized reflection coefficient contains a sign error [3], which leads to the incorrect conclusion. Equation (51) of Chapter 2 in [2] as it apparently should appear is given by

$$
\begin{aligned}
R_{V(SPM)} = {} & \\
& R_{V0} - k_{zi}\frac{k_1^2-k^2}{(k_1^2k_{zi}+k^2k_{1zi})^2}k^2k_1^2\sigma^2l^2\int_0^\infty e^{-(k_\rho^2+k_{\rho i}^2)l^2/4} \\
& \left\{k_{1zi}\left(I_0(x)-2\frac{k_\rho k_{\rho i}}{k_\rho^2+k_z k_{1z}}I_1(x)\right)\right. \\
& -\frac{k_1^2-k^2}{k_z+k_{1z}}\frac{k_{1zi}^2}{k_1^2}I_0(x)+\frac{k_1^2-k^2}{k_z+k_{1z}}\frac{k_\rho^2}{k_\rho^2+k_z k_{1z}}\frac{k_{\rho i}^2}{k^2}I_0(x) \\
& \left.+\frac{k_1^2-k^2}{k_z+k_{1z}}\frac{k_{1zi}^2}{k_1^2}\frac{k_\rho^2}{k_\rho^2+k_z k_{1z}}\left(I_0(x)-\frac{I_1(x)}{x}\right)\right\}k_\rho dk_\rho \qquad (1)
\end{aligned}
$$

where $x=\frac{1}{2}k_\rho k_{\rho i}l^2$, $R_{V(SPM)}$ is the vertical small perturbation Fresnel reflection coefficient, R_{V0} is the vertical Fresnel reflection coefficient for a plane interface, σ is the rms surface height, l is the surface correlation length, k, k_1 are the wavenumbers in the incident and other medium, respectively, $k_{zi}=k\cos\theta_i$, $k_{1zi}=\sqrt{k_1^2-k^2\sin^2\theta_i}$, $k_{\rho i}=k\sin\theta_i$, $k_z^2=k^2-k_\rho^2$, $k_{1z}^2=k_1^2-k_\rho^2$, θ_i is the angle of incidence and $I_n(x)$ is the modified Bessel function of order n. A Gaussian surface height distribution and a Gaussian correlation function have been assumed. The change in sign is on the second to last term in the integrand (which is the last term in [2]).

It is interesting to note that while the SPM expressions given by Tsang *et al.* [2] and Baylard *et al.* [4] for the H–polarization reflection coefficient agree to order σ_2, our translation of Baylard's SPM expression for the V-polarized reflection coefficient (to order

Manuscript received July 18, 1994; revised October 3, 1994.

The authors are with the The Radiation Laboratory, Department of Electrical Engineering and Computer Science, University of Michigan, Ann Arbor, MI 48109-2122 USA.

IEEE Log Number 9408265.

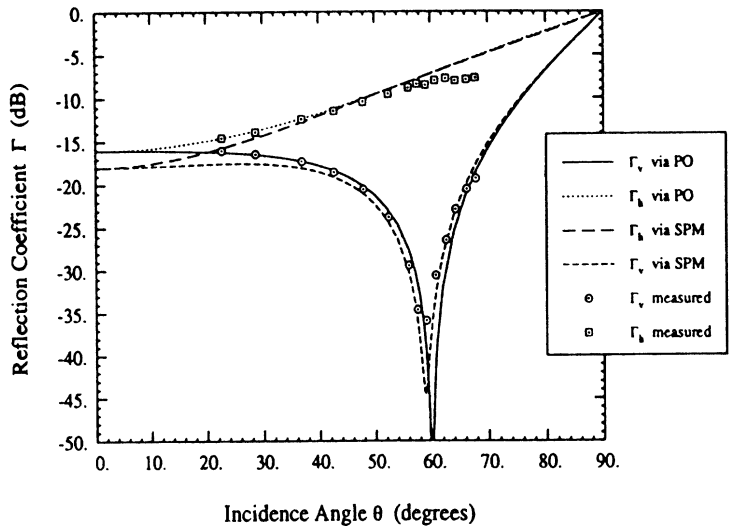

Fig. 1. Measured rough surface reflectivities compared to various theoretical expressions. $k\sigma = 0.515, kl = 5.4, \epsilon = 3.0 + j0, \Gamma_{v,h} = |R_{V,H}|^2$.

σ_2) into the above notation is as follows

$$R_{V(SPM)} = R_{V0} - k_{z1}\frac{k_1^2 - k^2}{(k_1^2 k_{z1} + k^2 k_{1z1})^2} k^2 k_1^2 \sigma^2 l^2 \int_0^\infty e^{-(k_\rho^2 + k_{\rho 1}^2) l^2/4} \left\{ k_{1z1}\left(\frac{k_1^2 - 2k_{\rho 1}^2}{k_1^2} I_0(x) - 2\frac{k_\rho k_{\rho 1}}{k_\rho^2 + k_z k_{1z}} \frac{k_1^2 - k^2}{k_z + k_{1z}} \frac{k_z}{k_1^2} I_1(x) \right) - \frac{k_1^2 - k^2}{k_z + k_{1z}} \frac{k_{1z1}^2}{k_1^2} I_0(x) + \frac{k_1^2 - k^2}{k_z + k_{1z}} \frac{k_\rho^2}{k_\rho^2 + k_z k_{1z}} \frac{k_{\rho 1}^2}{k^2} I_0(x) + \frac{k_1^2 - k^2}{k_z + k_{1z}} \frac{k_{1z1}^2}{k_1^2} \frac{k_\rho^2}{k_\rho^2 + k_z k_{1z}} \left(I_0(x) - \frac{I_1(x)}{x} \right) \right\} k_\rho dk_\rho. \quad (2)$$

The expressions are very similar, but not identical. Fortunately, the differences are numerically insignificant.

Fig. 1 shows the reflectivity of one of the surfaces we measured compared to the correct expression for SPM, as well as the predictions of physical optics (PO). It is clear that our data agrees with the prediction of SPM, including the shift of the Brewster angle toward nadir, for this slightly rough case. To the extent that we may have misrepresented the works of Greffet or Saillard [5], [6], we apologize.

We are pleased that our observations, at least for slightly rough surfaces, have a rigorous explanation. Unfortunately, a number of the rough surfaces that we have measured have roughnesses sufficiently large that they fall outside of the accepted range of validity for the SPM. The region of validity for the PO approach does encompass the roughnesses of the surfaces in our paper, and for this reason we emphasized that approach in the analysis of the entire body of data which we presented. Nonetheless, PO does not predict any shift of the Brewster angle, and the SPM is perhaps more appropriate for a detailed analysis of this phenomenon.

REFERENCES

[1] R. D. De Roo and F. T. Ulaby, "Bistatic specular scattering from rough dielectric surfaces," *IEEE Trans. Antennas Propagat.*, vol. 42, no. 2, pp. 220–231, Feb. 1994.

[2] L. Tsang, J. A. Kong, and R. T. Shin, *Theory of Microwave Remote Sensing*. New York: Wiley-Interscience, 1985.

[3] L. Tsang, private communication, Sept. 1994.

[4] C. Baylard, J.-J. Greffet, and A. A. Maradudin, "Coherent reflection factor of a random rough surface: Applications," *J. Opt. Soc. Amer. A*, vol. 10, pp. 2637–2647, Dec. 1993.

[5] M. Saillard and D. Maystre, "Scattering from metallic and dielectric rough surfaces," *J. Opt. Soc. Amer. A*, vol. 7, no. 6, pp. 982–990, June 1990.

[6] J.-J. Greffet, "Theoretical model of the shift of the Brewster angle on a rough surface," *Opt. Lett.*, vol. 17, no. 4, pp. 238–240, Feb. 1992.

Correction to "A Study of Transient Radiation from the Wu-King Resistive Monopole—FDTD Analysis and Experimental Measurements"

James G. Maloney and Glenn S. Smith

The above paper[1] contained the following errors. Equation (4) should read

$$\sigma_0 = \frac{(h/a_m)}{d\zeta_0 t'_0}$$

and in the first paragraph of Section III, $\sigma_0 d\zeta_0$ should equal 8.45, not 1.34. Equation (10) should read

$$\sigma = \frac{1}{2\pi a_m d\overline{r^i}}.$$

The correct expressions were used in all calculations so all of the numerical results, figures and tables in the paper are correct.

Manuscript received September 16, 1994.

The authors are with the Georgia Institute of Technology, Atlanta, GA 30332 USA.

IEEE Log Number 9408252.

[1] J. G. Maloney and G. S. Smith, *IEEE Trans. Antennas Propagat.*, vol. 41, no. 5, pp. 668–676, May 1993.